INVESTIGAÇÃO, CONSTRUÇÃO E DIFUSÃO DO CONHECIMENTO EM MATEMÁTICA
2

AMÉRICO JUNIOR NUNES DA SILVA
ANDRÉ RICARDO LUCAS VIEIRA
MIRIAN FERREIRA DE BRITO
(ORGANIZADORES)

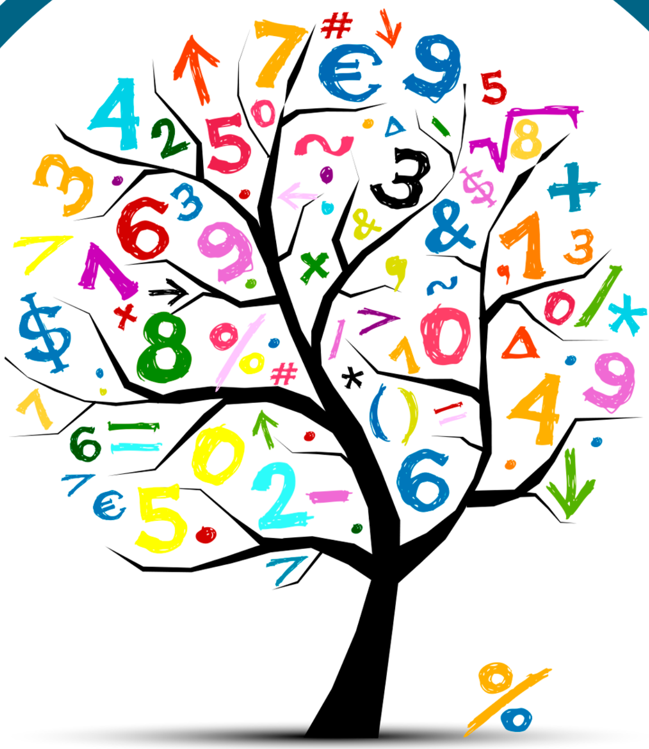

Atena Editora
Ano 2020

INVESTIGAÇÃO, CONSTRUÇÃO E DIFUSÃO DO CONHECIMENTO EM MATEMÁTICA 2

AMÉRICO JUNIOR NUNES DA SILVA
ANDRÉ RICARDO LUCAS VIEIRA
MIRIAN FERREIRA DE BRITO
(ORGANIZADORES)

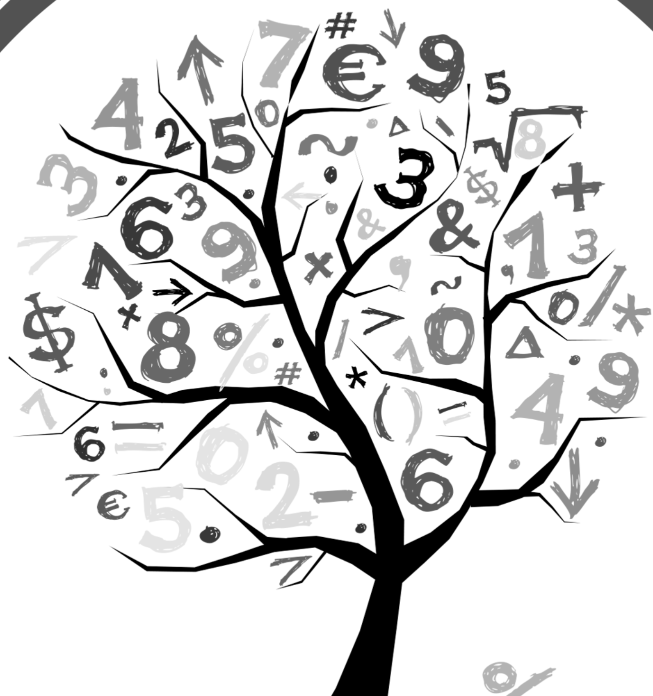

Atena Editora
Ano 2020

Editora Chefe
Profª Drª Antonella Carvalho de Oliveira
Assistentes Editoriais
Natalia Oliveira
Bruno Oliveira
Flávia Roberta Barão
Bibliotecária
Janaina Ramos
Projeto Gráfico e Diagramação
Natália Sandrini de Azevedo
Camila Alves de Cremo
Luiza Alves Batista
Maria Alice Pinheiro
Imagens da Capa
Shutterstock
Edição de Arte
Luiza Alves Batista
Revisão
Os Autores

Ciências Exatas e da Terra e Engenharias

Atena Editora
Ano 2020

Atena Editora
Ano 2020

Ciências Exatas e da Terra e Engenharias

Ciências Exatas e da Terra e Engenharias

Atena Editora
Ano 2020

Ciências Exatas e da Terra e Engenharias

Investigação, construção e difusão do conhecimento em matemática 2

Editora Chefe: Profª Drª Antonella Carvalho de Oliveira
Bibliotecária: Janaina Ramos
Diagramação: Camila Alves de Cremo
Correção: Vanessa Mottin de Oliveira Batista
Edição de Arte: Luiza Alves Batista
Revisão: Os Autores
Organizadores: Américo Junior Nunes da Silva
André Ricardo Lucas Vieira
Mirian Ferreira de Brito

Dados Internacionais de Catalogação na Publicação (CIP)

I62 Investigação, construção e difusão do conhecimento em matemática 2 / Organizadores Américo Junior Nunes da Silva, André Ricardo Lucas Vieira, Mirian Ferreira de Brito. – Ponta Grossa - PR: Atena, 2020.

Formato: PDF
Requisitos de sistema: Adobe Acrobat Reader
Modo de acesso: World Wide Web
Inclui bibliografia
ISBN 978-65-5706-610-2
DOI 10.22533/at.ed.102201012

1. Matemática. 2. Conhecimento. I. Silva, Américo Junior Nunes da (Organizador). II. Vieira, André Ricardo Lucas (Organizador). III. Brito, Mirian Ferreira de (Organizadora). IV. Título.

CDD 510

Elaborado por Bibliotecária Janaina Ramos – CRB-8/9166

Atena Editora
Ponta Grossa – Paraná – Brasil
Telefone: +55 (42) 3323-5493
www.atenaeditora.com.br
contato@atenaeditora.com.br

Atena Editora
Ano 2020

DECLARAÇÃO DOS AUTORES

Os autores desta obra: 1. Atestam não possuir qualquer interesse comercial que constitua um conflito de interesses em relação ao artigo científico publicado; 2. Declaram que participaram ativamente da construção dos respectivos manuscritos, preferencialmente na: a) Concepção do estudo, e/ou aquisição de dados, e/ou análise e interpretação de dados; b) Elaboração do artigo ou revisão com vistas a tornar o material intelectualmente relevante; c) Aprovação final do manuscrito para submissão.; 3. Certificam que os artigos científicos publicados estão completamente isentos de dados e/ou resultados fraudulentos.

Ciências Exatas e da Terra e Engenharias

Atena Editora

Ano 2020

APRESENTAÇÃO

O contexto social, histórico e cultural contemporâneo, fortemente marcado pela presença das Tecnologias Digitais de Informação e Comunicação – TDIC, entendidas como aquelas que têm o computador e a internet como instrumentos principais, gera demandas sobre a escola e sobre o trabalho docente. Não se trata de afirmar que a presença das tecnologias na sociedade, por si só, justifica sua integração à educação, mas de considerar que os nascidos na era digital têm um perfil diferenciado e aprendem a partir do contexto em que vivem, inclusive fora da escola, no qual estão presentes as tecnologias.

É nesta sociedade altamente complexa em termos técnico-científicos, que a presença da Matemática, alicerçada em bases e contextos históricos, é uma chave que abre portas de uma compreensão peculiar e inerente à pessoa humana como ser único em sua individualidade e complexidade, e também sobre os mais diversos aspectos e emaranhados enigmáticos de convivência em sociedade. Convém salientar que a Matemática fornece as bases do raciocínio e as ferramentas para se trabalhar em outras ciências. Faz-se necessário, portanto, compreender a importância de se refletir sobre as estratégias pedagógicas utilizadas no ensino desta ciência.

Ensinar Matemática não se limita em aplicação de fórmulas e regras, memorização, aulas expositivas, livros didáticos e exercícios no quadro ou atividades de fixação, mas necessita buscar superar o senso comum através do conhecimento científico e tecnológico. Importante, nos processos de ensino e aprendizagem matemática priorizar e não perder de vista o prazer da descoberta, algo peculiar e importante no processo de matematizar. Isso, a que nos referimos anteriormente, configura-se como um dos principais desafios do educador matemático.

A prática pedagógica intrínseca ao trabalho do professor é complexa, e buscar o “novo” exige o enfrentamento de situações inusitadas. Como a formação inicial representa a instância formadora dos esquemas básicos, a partir dos quais são desenvolvidas outras formas de atuação docente, urge analisá-la a fundo para identificar as problemáticas que implicam diretamente no movimento de profissionalização do professor que ensina matemática.

É neste sentido, que o livro “***Investigação, Construção e Difusão do Conhecimento em Matemática***”, em seu *volume 2*, reúne trabalhos de pesquisa e experiências em diversos espaços, como a escola por exemplo, com o intuito de promover um amplo debate acerca das variadas áreas que o compõe.

Por fim, ao levar em consideração todos esses elementos, a importância desta obra, que aborda de forma interdisciplinar pesquisas, relatos de casos e/

ou revisões, refletem-se nas evidências que emergem de suas páginas através de diversos temas que suscitam não apenas bases teóricas, mas a vivência prática dessas pesquisas.

Nessa direção, portanto, desejamos a todas e a todos uma boa leitura!

Prof. Dr. Américo Junior Nunes da Silva
Prof. Me. André Ricardo Lucas Vieira
Profa. Dra. Mirian Ferreira de Brito

SUMÁRIO

CAPÍTULO 1

MATHEMATICAL MODELING AND BIDIMENSIONAL SIMULATION OF THE NAVIER-STOKES EQUATIONS FOR TURBULENT FLOW IN INCOMPRESSIBLE NEWTONIAN FLUIDS AROUND ISOTHERMAL GEOMETRIES

Data de aceite: 17/11/2020
Data de submissão: 06/10/2020

Rômulo Damasclin Chaves dos Santos
Postdoctoral Researcher Fellow
Campinas State University – UNICAMP/SP
Campinas, São Paulo
http://lattes.cnpq.br/5416661457556148

ABSTRACT: An immersed boundary method is development for the fluid-body interaction, being consider the heat-transfer for the onset turbulence in two-dimensional (2D) thermofluid dynamics around isothermal complex geometries immersed in incompressible Newtonian flows. The fluid motion and temperature are defined on a fixed Eulerian grid, while the immersed body is defined on a Lagrangian grid. A virtual physical model is used for the diffusion of interfacial forces within the flow, guarantees the imposition of the no-slip boundary condition. This model dynamically evaluates not only the force that the fluid exerts on the solid surface, but the heat exchange between them. Therefore, this work presents the Navier-Stokes equations, together with the energy equation, under physically appropriate boundary conditions. To calculate the turbulence viscosity, two models where used, to know, the Smagorinsky model, implemented in the context of the Large Eddy Simulation (LES) model, and Spalart-Allmaras model, based on Unsteady Reynolds Average Navier-Stokes Equation (URANS). For all simulations, a computational code was developed to calculate different dimensionless numbers, such as, lift and drag coefficients, Nusselt, Strouhal numbers, among other. The results are compared with previous numerical results, considering different Reynolds numbers.
KEYWORDS: Immersed Boundary Method, Mixed Convection, Laminar and Turbulent Flow.

1 I INTRODUCTION

Many physical phenomena in fluid mechanics can be describe by mathematical modeling, using a set of partial differential equations, often nonlinear, known as the laws of conservation of fluid mechanics, they are: conservation of momentum, conservation of mass (continuity) and energy. These laws together model the dynamics of the forces acting on the fluid, as well as, the energy exchange that occurs in the different regions of the flow. In this work, this set of equations was discretized by finite difference method, for incompressible Newtonian fluid, where it relates the term of viscous stresses with the deformation rates in the velocity field, thus simulating the flow dynamics with the called Navier-Stokes equation.

Traditional methods of domain discretization present some difficulty in terms of implementation and calculation time, requiring successive remeshing process (reconstruction of new mesh) for each new iterative process, in addition to the need to introduce a new generalized coordinate system. Thus, considering these physical and mathematical problems, a computational code was developed for the immersed boundary methodology for the thermofluid dynamics interaction. We present some of the main works involving the immersed boundary method, considering the heat-transfer by mixed convection process. The purpose of this set of references is the preparation for the theoretical foundation of the methodology, bringing greater ease with respect to the immersed boundary methodology, extracting important physical and mathematical conceptual points, which will be applied in the methodology of interest in this work. Among the main references involving the thermal part, we can list some important ones, such as, Badr & Dennis (1985) and Badr *et al*. (1990). These works do not present the immersed boundary method, but they are an excellent precursor in relation to the flow around rotating circular cylinder involving forced convection, being the theoretical basis used in other important works for the implementation of the thermal part. In summary, the experimental and numerical works of the authors Badr & Dennis considered the problem of laminar flow with heat-transfer by forced convection from a rotating circular cylinder around its own axis, initially for a Reynolds number equal to 100, with a specific rotation rate (α), for the interval varying between $0.5 \leq \alpha \leq 3.0$. Meanwhile, the second work, uses the Reynolds number range varying between $10^3 \leq Re \leq 10^4$, with specific rotation rate equal to 4. In both works, the cylinder is located in a uniform flow. Thus, the author report that the temperature fields are strongly influenced by the vorticity of rotation of the cylinder. The author found, in both studies, that the heat-transfer coefficient tends to decrease as the rotation of the cylinder increase. An attribution of the presence of a layer of rotating fluid around the cylinder was verified, being separated from the main flow of the flow. Thus, the results demonstrated convergence and numerical stability compared to others available in the literature (see, Lai & Peskin (2006) and Sharma *et al*. (2012))

Park et al. (2017), present the immersed boundary method developed for the study of fluid and flexible body interactions with heat transfer. The movement of the fluid and the temperature are defined in a fixed Eulerian grid, while the flexible movement of the body is defined in a mobile Lagrangian grid. The governing equations for fluid movement, temperature and flexible body movement are solved independently in each grid. To deal with the transfer of momentum between the flexible body and the fluid, a forcing term is added to the fluid motion equations with the imposition of the non-slip condition of the fluid in the flexible body. A heat source is added between the heated body and the surrounding fluid, which can be calculated in a similar way to that used to obtain the amount of movement, imposing the thermal conditions on the body. The momentum and heat transformation between the Eulerian and Lagrangian variables were established using the Dirac delta function. To validate the methodology used by Park et al. (2017), the problems of natural and forced convection for a rigid circular cylinder were simulated. For the natural convection of the heated rigid cylinder with the isothermal boundary condition, a good approximation with the reference data was obtained. For forced convection, a flow around the rigid circular cylinder was also simulated with both isothermal and constant heat flow boundary conditions. The Nusselt average local number for the cylinder, obtained good convergence in relation to the scientific literature. Finally, a flow around the heated flexible cylinder was simulated, and the heat transfer was evaluated in comparison with the rigid cylinder. Two different states were observed for the flexible cylinder, depending on the number of Reynolds and the flexible characteristic of the cylinder. For $Re = 10$ and $Re = 20$, the cylinder presented the "extended-stable" state regardless of the flexible property, where the heat transfer was deteriorated in relation to the rigid cylinder. The flexible variation experienced an initial circular shape to a fan-shape in the extended-stable state. Longitudinal elongation increases the Nusselt number near the fixed point, but decreased the transverse thermal dissipations upstream of the cylinder to the aerodynamic shape rather than circular, this resulted in a decrease in the Nusselt number. Other analyzes were performed and validate, including stability for the fluid-body interaction constants and heat transfer. The problems of natural and forced convection with the boundary condition of the thermal and isothermal flow are simulated with a good approximation compared to previous studies. At $Re = 40$, the cylinder showed both behaviors, depending on the flexible property. Other analyzes were performed and validated, including stability for the fluid-body interaction constants and heat transfers. The problems of natural and forced convection with the boundary conditions of the thermal and isothermal flow are simulated with a good approximation compared to previous studies. Simulations for heat transfer by forced convection around a flexible circular cylinder have been made and validated.

Santos *et al.* (2018), presented the immersed boundary method coupled with virtual physical model to simulated incompressible two-dimensional flows around a heated square cylinder at constant temperature on its surface. A good numerical convergence was obtained, being the margin of error, with respect to the works, less than 3%. The time evolution of the drag and lift coefficient, as well as, the Nusselt number were obtained with this methodology, being the parameters obtained from the Eulerian fields, since the geometry used in this work has singularities, which were taken into account in the construction of the code. The implementation process for the calculation of the drag and lift coefficients is simple. This fact is important, because it allows its applicability to other (less simple) geometries. In all simulations, the results show that influence of the surface of the heated body immersed in the flow increase as the Reynolds numbers increase. For the temporal discretization, the second-order Adams-Bashforth scheme was used together with spatial centered scheme. The considered turbulence models were used for the energy transfer process between the largest and the smallest turbulent scales.

In addition to the validation of the methodology, another objective was to better understand all the phenomena present in this flow through a two-dimensional analysis, evaluating the thermal influence of the cylinder on the flow, the emission of vortices and the dynamics of formation and suppression of the wake. The influence of rotation on reducing drag and increasing the lift coefficient was verified, as well as, the distribution of the thermal field near the cylinder. With the rotation movement, the vortex wake is displaced in relation to the horizontal flow line. With the increase of the rotation, the amplitude of oscillations of the fluid dynamic coefficients, tend a null value, that is, the process of vortex generation tends to decrease with the increase of the specific rotation value. Finally, it was verified that the number of Strouhal is little influence for basic values of the specific rotation, but that it depends on the number of Reynolds. The quantitative results show a good numerical agreement in relation to the results available in the literature. Based on this, the immersed boundary methodology with the virtual physical model proved to be promising for the flow simulation with forced convection.

In this work, the properties were considered constant. The buoyance term is based on the approximation of the Boussinesq approximation, considering the problems of mixed convection. Other terms, such as, energy generation, are neglected in this work, as well as, internal heat or humidity. Coriolis force or rotation effects are also absent in this work. The proposed methods were validated for natural and forced convections with the isothermal and constant heat flux boundary conditions. Finally, the heat transfer and the onset turbulence around complex geometry with the surrounding fluid was examined. The obtained numerical results are accurate and stable, presenting a good agreement with the available results in the literature. The following section presents the mathematical methodology.

2 | MATHEMATICAL METHODOLOGY

2.1 Formulation for the fluid motion and temperature

Considering an incompressible and two-dimensional flow a Newtonian fluid, with a domain represented by Ω, and a boundary represented by $\partial\Omega$, with the surface of the immersed body being heated with constant temperature, which can be modeled through discretized points, previously named by Lagrangian points. Since the effect of the frontier is taken into account through the introduction of the forcing term in the momentum and energy equation, the equations that describe the heat transfer by mixed convection in the immersed boundary methodology are expressed as follows

$$\nabla \cdot \mathbf{u}\,, \tag{1}$$

$$\rho_0\left(\frac{\partial \mathbf{u}}{\partial t} + (\mathbf{u}.\nabla)\mathbf{u}\right) = -\nabla p + \mu\nabla^2\mathbf{u} + \mathbf{f}\,, \tag{2}$$

$$\rho_0\left(\frac{\partial \mathbf{u}}{\partial t} + (\mathbf{u}.\nabla)\mathbf{u}\right) = -\nabla p + \mu\nabla^2\mathbf{u} + \rho_0\mathbf{g}\big(1-\beta(T-T_\infty)\big)\mathbf{j} + \mathbf{f}\,, \tag{3}$$

$$\rho_0 c_p\left(\frac{\partial T}{\partial t} + (\mathbf{u}\,.\nabla)T\right) = k\nabla^2 T + q\,, \tag{4}$$

Where Eqs. (1), (2) and (4) are forced convection, while Eqs. (1), (3) and (4) are for natural convection, and in Eq. (3), the Boussinesq approximation is used. The terms, **u,** p, T and T_∞ denote, velocity vector, pressure, temperature and reference temperature, respectively. The terms, ρ_0, μ, β, k and c_p are fluid density at temperature $T = T_\infty$, viscosity, thermal diffusivity, thermal expansion coefficient and specific heat at constant pressure, **g** is a downward gravitational acceleration; the term $\rho_0\, \mathbf{g}\, (1\text{-}\beta(T\text{-}T_\infty))$ accounts for the effects of the fluid temperature on the fluid flow, the term **j** is the unit vector in the positive y-axis direction, respectively.

The term of force **f** and thermal source q in the Eqs. (2) e (3) are the Euler force fields where these sources model the existence of the interface immersed in the flow, visualizing the body immersed in the flow having non-null value in Eulerian grid near the Lagrangian grid, being expressed by

$$\mathbf{f}(x,t) = \int_{\partial\Omega_b} F(\mathbf{X}_k,t)\delta(x-\mathbf{X}_k)d\mathbf{X}_k\,, \tag{5}$$

where $F(\mathbf{X}_k,t)$ is the Lagrangian force density, calculated on the interface points x and $\mathbf{X}_k$ which are the positions of a particle of Eulerian and Lagrangian fluid on the interface, respectively. The term $\delta(x - \mathbf{X}_k)$ is the Dirac delta function, which represents the interaction between the fluid and the immersed boundary. Similarly, the thermal source represented by q is added to Eq. (4), being responsible for making the flow feel the presence of the heated solid interface, in other words, it is heating source at the Lagrangian point on the immersed border, being able to be expressed by

$$q(x,t) = \int_{\partial\Omega_b} Q(\mathbf{X}_k,t)\delta(x-\mathbf{X}_k)d\mathbf{X}_k\,, \tag{6}$$

where, $Q(\mathbf{X}_k,t)$ is the heat flux at the border being the difference between the derivative of the approximate specific temperature.

2.2 The virtual physical model

The virtual physical model, developed by Silva *et at*. (2003), is a methodology for calculating the forces that act on the discrete points of a given border, also called the interfacial force or Lagrangian force. The characterization of the Lagrangian force represents the difference between the various immersed boundary methodologies. In this work, only the rigid boundaries were treated (no elasticity), but the model can be used or extended to other types of interface, for example, for elastic boundaries, boundaries between different fluids, etc. The virtual physical model uses the diffusion of interfacial forces on the interior of the flow. Thus, the Eulerian force field is applied in the vicinity of the immersed boundary, and its value is minimized as the distance to the interface increases. This model dynamically assesses not only the force that the fluid exerts on the solid surface immersed in the flow, bur takes into account the thermal exchange between them.

The Lagrangian force $F(\mathbf{X}_k, t)$, and the thermal source $Q(\mathbf{X}_k, t)$, are evaluated separately, in other words, for Lagrangian force a balance of amount of movement was carried out on a fluid particle that in close to the fluid-solid interface, while for the thermal part, the dimensionless energy equation was applied, which shows the interaction between the particle fluid and the interface, which takes into account all the terms of the Navier-Stokes equation. Then, assuming that all particle fluid, including those over the interface, must satisfy the balance of amount of movement and energy. Thus, the density of interfacial force can be evaluated using the principle of conservation of the momentum and energy, applying over any participle of fluid that makes up the flow. Therefore, taking the particle fluid crossing an arbitrary immersed boundary interface, we obtain the following formulation

$$F(\mathbf{X}_k, t) = \underbrace{\rho \frac{\partial \mathbf{U}(\mathbf{X}_k, t)}{\partial t}}_{F_a} + \underbrace{\rho \, \nabla[\mathbf{U}(\mathbf{X}_k, t)\mathbf{U}(\mathbf{X}_k, t)]}_{F_i} + \underbrace{\nabla p(\mathbf{X}_k, t)}_{F_p} - \underbrace{\mu \nabla^2(\mathbf{X}_k, t)}_{F_v} , \tag{7}$$

where, the portions referring to the terms of the Eq. (7), from left to right, are called acceleration force, inertial force, pressure force and viscous force, respectively.

In a manner similar to that performed in Eq. (7), for the calculation of the thermal source in the particle fluid in contact with the interface, an energy balance is performed as follows

$$Q(\mathbf{X}_k, t) = \frac{\partial \Theta(\mathbf{X}_k, t)}{\partial \mathrm{t}} + \nabla[\mathbf{U}(\mathbf{X}_k, t)\Theta\mathbf{U}(\mathbf{X}_k, t)] - \frac{1}{Pe}\nabla^2\Theta(\mathbf{X}_k, t) , \tag{8}$$

where, the portions referring to Eq. (8), from de right, are called local temperature variation rate, thermal dissipation rate due to convection and diffusive thermal energy transport rate. In Eq. (8), each term is evaluated based on the values of the variables (velocity, pressure and temperature), of the Eulerian grid, interpolated for the Lagrangian grid and for the auxiliary points used in obtaining spatial derivatives. This process is detailed in the next subsection.

2.3 Calculation of velocity, pressure and temperature

2.3.1 Auxiliary point allocation process

The first step is to arbitrate an initial Lagrangian point for calculating the interfacial force $F(\mathbf{X}_k, t)$. Then, two mutually orthogonal auxiliary lines are drawn on this point, one of which is parallel to one of the Eulerian axes. Two auxiliary points are marked on each of the lines, on the outside of the solid body, at a distance Δx and 2 Δx of the Lagrangian point considered. This distance is necessary in order to prevent two auxiliary points from being allocated within the same Eulerian cell. The grids that are more that 2 Δx distance from the Lagrangian points, do not contribute to the interpolation. The internal and external regions of the solid body were identified with the aid of the normal unitary vector on the surface, which has its positive direction forcing outside the immersed body. The auxiliary points are always located in the regions of interest of the flow, that is, in the region to be simulated. Thus, the values of velocity, pressure and temperature at the points, in general, are not know, but can be obtained, from neighboring cells, with the ais of a distribution/interpolation function.

Thus, the general equation for obtaining the velocity at Lagrangian points and auxiliary points is expressed in the following formula

$$\mathbf{U}(\mathbf{X}_k) = \sum_i D_i(x_i - \mathbf{X}_k)\, \mathbf{U}(x_i)\,, \tag{9}$$

where $\mathbf{U}(\mathbf{X}_k)$ are the Lagrangian velocities, calculated at the auxiliary points and at the point $\mathbf{X}_k$ by the interpolation of the Eulerian velocities. Similarly, for the calculation of pressure and temperature derivatives at each Lagrangian point, it was necessary to obtain the pressure and temperature values on the interface, at point $\mathbf{X}_k$. Thus, for the calculation of pressure and temperature an auxiliary point, which is in a normal position at a distance Δx from the Lagrangian point. The general equation for obtaining the pressure and temperature at the auxiliary points or on the interface and at the Lagrangian points in the x and y directions are given, respectively, by the systems

$$p(\mathbf{X}_k) = \sum_i D_i(x_i - \mathbf{X_k})\, p(x_i) \qquad (10)$$

$$\Theta(\mathbf{X}_k) = \sum_i D_i(x_i - \mathbf{X_k})\, \Theta(x_i)$$

$$p(\mathbf{Y}_k) = \sum_i D_i(x_i - \mathbf{Y_k})\, p(y_i) \qquad (11)$$

$$\Theta(\mathbf{Y}_k) = \sum_i D_i(x_i - \mathbf{Y_k})\, \Theta(y_i)$$

where, $p(\mathbf{X}_k)$ and $p(\mathbf{Y}_k)$ are pressure values on the interface, and $p(y_i)$ and $p(x_i)$ are pressure value in the nearest Eulerian grids, in the x and y directions, respectively. Similarly, $\Theta(\mathbf{X}_k)$ and $\Theta(\mathbf{Y}_k)$ are the temperatures at auxiliary points at k points and $\Theta(x_i)$, the temperature at the nearest Eulerian points. The distribution/interpolation function D, adopted in thus work, is used for the interpolation of variables in the Eulerian grid. Regarding the computational cost involved, it was reduced when considering non-null D for distances less than $2\Delta x$ from the interpolation point, which is also valid for the $F(\mathbf{X}_k,t)$ distribution. Therefore, in this work, Peskin (1977) proposal, modified by Juric (1996), is used, being defined by

$$D(x-\mathbf{X_k}) = \prod_{m=1}^{N} \frac{g(r_x)g(r_y)}{h^2}, \tag{12}$$

where,

$$g(r) = \begin{cases} g_1(r) & , if \quad \|r\| < 1 \\ 0.5 - g_1(2-\|r\|) & , if \quad 1 < \|r\| < 2 \\ 0 & , if \quad \|r\| > 2 \end{cases} \tag{13}$$

where, $g_1(r) = {}^1/_8\left(3 - 2\|r\|\sqrt{1+4\|r\|-4\|r\|^2}\right)$, and r is called the radius of influence of the distribution function, being represented here by $\left[\frac{1}{h}(x-x_k)\right]$ or $\left[\frac{1}{h}(y-y_k)\right]$. The term, $h = \Delta x = \Delta y$, is the size of the Eulerian grid and (x,y) the coordinates of a Eulerian point in the domain. To calculate the temperature at each time step in the iterative process over the immersed boundary, the following equation was used

$$\Theta(\mathbf{X}_k) = \sum_i D_i(x_i - \mathbf{X}_k)\,\Theta(x_i)\,. \tag{14}$$

Thus, after the interpolation of velocity, pressure and temperature at the interface and at auxiliary points, the derivatives that make up the terms for the calculation of Lagrangian source terms are determined in the x and y directions, with the so-called Lagrange polynomials of first and second order. Generically, denominated the components of velocity or pressure, defined by the interpolation function ϕ, given by the linear combination of the Lagrange polynomials, in the form

$$\phi(x) = \sum_{i=0}^{m} \phi_i \prod_{j=0, j\neq i}^{m} \frac{x - x_j}{x_i - x_j}\,. \tag{15}$$

2.3.2 Calculation of Lagrangian force distribution and thermal source

After calculating the terms das Eqs. (7) and (8), and obtaining the values for $F(\mathbf{X}_k,t)$ and $Q(\mathbf{X}_k,t)$, then the Eulerian terms are calculated for $\mathbf{f}$ and q. The system calculation for the terms **f** and *q*, in the x and *y* direction, are presented below, respectively

$$\mathbf{f}(x_i) = \sum_i D_i\,(x_i - \mathbf{X}_k)\,F(\mathbf{X_k})\,\Delta s\,(\mathbf{X}_k)$$
$$\mathrm{q}(x_i) = \sum_i D_i\,(x_i - \mathbf{X}_k)\,Q(\mathbf{X_k})\,\Delta s\,(\mathbf{X}_k) \tag{16}$$

$$\mathbf{f}(y_i) = \sum_i D_i\,(y_i - \mathbf{Y}_k)\,F(\mathbf{Y_k})\,\Delta s\,(\mathbf{Y}_k)$$
$$\mathrm{q}(y_i) = \sum_i D_i\,(y_i - \mathbf{Y}_k)\,Q(\mathbf{Y_k})\,\Delta s\,(\mathbf{Y}_k) \tag{17}$$

where, in the Eqs. (16) and (17), in the respective x and *y* directions, $\mathbf{f}(x_i)$ and $\mathbf{f}(y_i)$, are the forces at each Eulerian node, while $F\,(\mathbf{X}_k)$ and $F\,(\mathbf{Y}_k)$, are the force in each Lagrangian node being distributed to Eulerian nodes. The terms, $\mathrm{q}(x_i)$ and $\mathrm{q}(y_i)$, is presented are heat sources for each Eulerian node, due the presence of immersed heated, and $Q\,(\mathbf{X}_k)$ and $Q\,(\mathbf{Y}_k)$ are the thermal source in each Lagrangian node being distributed to the nodes Eulerian, thus forming, a thermal field of Eulerian force that acts on the fluid particles near the border.

3 I MATHEMATICAL MODELING OF TURBULENCE

3.1 The Smagorinsky model

The algebraic modeling Smagorinsky (1963) is based on the local equilibrium hypothesis for small scales, so that the injected energy in the spectrum, defined by

$$\xi = -\overline{u'_\iota u'_J S_{\iota J}} = 2\nu \overline{S_{\iota J}}\,\overline{S_{\iota J}}\,, \tag{18}$$

Equals the dissipated energy by the viscous effects. The terms, u'_i and u'_j are, respectively, the characteristics scales of velocity of the sub-grid. It is assumed that the turbulent viscosity sub-grid is proportional to these characteristics scales, according to the equation

$$\nu_t = C_s \ell \left(u'_j u'_i\right)^{\frac{1}{2}}. \tag{19}$$

The turbulent viscosity, Eq. (19), can be expressed as a function of the strain rate tensor (S_{ij}), the characteristic length scale (ℓ), associated with the grid size and the C_s constant, called the Smagorinsky constant, the viscosity turbulent is then represented by

$$\nu_t = (C_s \ell)^2 \sqrt{2\bar{S}_{ij}\bar{S}_{ij}}\ , \tag{20}$$

where, the strain rate tensor $\bar{S}_{ij}$ is represented by

$$\bar{S}_{ij} = \frac{1}{2}\left(\frac{\partial \bar{u}_i}{\partial x_j} + \frac{\partial \bar{u}_j}{\partial x_i}\right), \quad (21)$$

where, the implementation related to the damping function was implemented in such a way as to dampen the turbulent viscosity close to the walls of the immersed boundary, regardless of the type of geometry to be considered.

3.2 The Spalart-Allmaras model

The Spalart-Allmaras turbulence model emerged in the 1990's after a coherent convergence between ideas about an empirical model that resolved the turbulence, that is, that which only a single equation, the modeling would occur directly, solving the question of the main turbulent parameter: turbulent viscosity, without involving calculations with turbulent energy or dissipation or vorticity, where in other existing models, these characteristic parameters are necessary to define the turbulence behavior in the flow. In the Spalart-Allmaras model, a transport equation for turbulent viscosity is established, using empiricism and argument from dimensional analysis, invariance and a selective dependence on molecular viscosity, according to the works of Spalart *et al.* (1992). The equation includes a non-viscous destruction term that depends on the distance to the wall. Unlike algebraic models, the first models of an equation are local, in the sense that the equation at one point does not depend on the solution at other points. Therefore, it is compatible with grids of any nature. The solution close to the wall is less difficult to obtain.

Wall and undisturbed flow conditions are elementary. The model produces relatively smooth turbulent laminar transition at points specified by the user. The model was calibrated in boundary layers with a pressure gradient. The turbulent viscosity (ν_t) is calculated from the Spalart-Allmaras working aid variable, $\tilde{\upsilon}$, and damped by the function f_{ν_1} near to the walls,

$$\upsilon_t = \tilde{\upsilon} f_{\upsilon_1}, \quad (22)$$

where,

$$f_{\upsilon_1} = \frac{\chi^3}{\chi + C_{\upsilon_1}^3}, \quad (23)$$

with,

$$\chi = \frac{\tilde{\upsilon}}{\upsilon}. \quad (24)$$

Thus, the so-called auxiliary work variable of the Spalart-Allmaras model, $\tilde{\upsilon}$, obeys the following transport equation

$$\frac{\partial \tilde{v}}{\partial t} + \frac{\partial}{\partial x_j}(u_j \tilde{v})$$

$$= c_{b_1}(1 - f_{t_2})\tilde{S}\tilde{v} + \frac{1}{\sigma}\left[\frac{\partial}{\partial x_j}\left((v + \tilde{v})\frac{\partial \tilde{v}}{\partial x_j}\right) + c_{b_2}\frac{\partial \tilde{v}}{\partial x_j}\frac{\partial \tilde{v}}{\partial x_j}\right] \quad (25)$$

$$- \left[c_w f_w - \frac{c_{b_1}}{k^2} f_{t_2}\right]\left[\frac{\tilde{v}}{d_w}\right]^2 + f_{t_1}\Delta U^2 ,$$

where the terms on the right side of Eq. (25) represent, respectively: (**i**) the production of turbulent viscosity, (**ii**) the molecular and turbulent diffusions of $\tilde{v}$, (**iii**) the dissipation of $\tilde{v}$, (**iv**) the destruction of $\tilde{v}$ that reduces the turbulent viscosity to the wall and, finally, (**v**) the terms that model transition effects to turbulence, indicated by the subindex *t*. For regions distant from the walls, the function f_{v_1} has no influence on the calculation of turbulent viscosity, being its unit value and, therefore, making $v_t = \tilde{v}$. The production term of the transport equation, Eq. (25), also needs a correction near to the wall, which is performed by replacing the parameter *S* with a modified variable $\tilde{S}$, which is also influenced by a damping function f_{v_2}, defined similarly to f_{v_2}. Thus, $\tilde{S}$ and f_{v_2} are presented below by following formulation

$$\tilde{S} = S + \frac{\tilde{v}}{(kd_w)^2} f_{v_2} , \quad (26)$$

$$f_{v_2} = 1 - \frac{\chi}{1 + \chi f_{v_1}}, \quad (27)$$

where, d_w, Eq. (26), is the distance to the near wall, and *S* is the modulus of the strain rate, calculated with the variables of the filtered field, being calculated by

$$S = \sqrt{2\bar{S}_{ij}\bar{S}_{ij}} . \quad (28)$$

The function f_w is defined as a unit values for the region of the logarithmic boundary layer, intensifying the term of distribution as it approaches the wall, tending to zero for the most distant regions of the wall, thus being defined as being

$$f_w = g\left(\frac{1 + c_{w_3}^6}{g^6 + c_{w_3}^6}\right), \quad (29)$$

where,

$$g = r + c_{w_2}(r^6 - r) , \quad (30)$$

and,

$$r \equiv \frac{\tilde{v}}{\bar{S}\, k^2 d_w^2}. \quad (31)$$

Others constants of the model are $\sigma = {}^2/_3$, $c_{b_1} = 0.1355$, $c_{b_2} = 0.622$,

$k = 0.41$, $c_{w_1} = {c_{b_1}}/{k^2} + {(1 + c_{b_2})}/{\sigma}$, $c_{w_2} = 0.3$, $c_{w_3} = 2$ and $c_{v_1} = 7.1$. These constants were determined empirically. Regarding the average energy equation with turbulent diffusivity, applying an additional scale Q_j, being represented by

$$\frac{\partial \bar{\Theta}}{\partial t} + \frac{\partial(\bar{u}_j \bar{\Theta})}{\partial x_i} = \frac{\partial}{\partial x_j}\left[\alpha\left(\frac{\partial \bar{\Theta}}{\partial x_j}\right) + \overline{u_j \Theta} - \bar{u}_j \bar{\Theta}\right], \tag{32}$$

where, the term $\bar{\Theta}$ is the resolved temperature field.

4 I NUMERICAL METHOD

The numerical method used in this paper is the fractional steps that unites the velocity and pressure. With the aim to solve the Navier-Stokes equation, result new velocity and pressure fields. For the time discretization is used Euler's method of the first order. The Navier-Stokes equation were solved explicitly. The correction of pressure results in a linear system, solved by Modified Strongly Implicit Procedure developed by Schneider & Zedan (1981). The Eq. (2), can be rewritten in the following in the following way

$$\frac{u_i^{n+1} - u_i^m}{\Delta t} + \left[\frac{\partial}{\partial x_j}(u_i^n u_j^n)\right] = -\frac{1}{\rho}\frac{\partial p^{n+1}}{\partial x_i} + \frac{\partial}{\partial x_j}\left[(v + v_t)\left(\frac{\partial u_i^n}{\partial x_j} + \frac{\partial u_j^n}{\partial x_i}\right)\right] + f_i^n . \tag{33}$$

In the fractional step method, the velocities, pressure and the forcing term of the predictive instant (n) are used to calculate, in the predictive step, and estimate for the velocity in the current time $\bar{u}_i^{n+1}$, represented by the equation

$$\frac{\bar{u}_i^{n+1} - u_i^m}{\Delta t} + \left[\frac{\partial}{\partial x_j}(u_i^n u_j^n)\right] = -\frac{1}{\rho}\frac{\partial p^{n+1}}{\partial x_i} + \frac{\partial}{\partial x_j}\left[(v + v_t)\left(\frac{\partial u_i^n}{\partial x_j} + \frac{\partial u_j^n}{\partial x_i}\right)\right] + f_i^n , \tag{34}$$

the next step in the fractional step method is to subtract Eq. (34) from Eq. (33), resulting in

$$\frac{\bar{u}_i^{n+1} - u_i^n}{\Delta t} = \frac{1}{\rho}\frac{\partial}{\partial x_i}(p^{n+1} - p^n) , \tag{35}$$

doing some algebraic manipulations, we get the pressure field calculated, we obtaining the equation corrected for the velocity in the current iteration (corrector step), being represented by

$$u_i^{n+1} = \bar{u}_i^{n+1} - \frac{\Delta t}{\rho}\frac{\partial p'^{n+1}}{\partial x_i} . \tag{36}$$

5 I RESULTS

Using the immersed boundary method coupled virtual physical model, implemented in C++ code, is possible perform simulation of (2D) (two-dimensional) flows around a heated body immersed in the flow. In this section, the flow around a pair of heated circular cylinders in tandem have equal diameters and the same center-to-center distance (L_{CC}). The fluid and the heat flow are characterized by Reynolds number $Re = \frac{\rho U_\infty D}{\mu}$ and Prandtl number $Pr = \frac{\mu c_p}{k}$, where ρ is the fluid density, U_∞ is the free stream velocity, D is the cylinder diameter, μ is the dynamic viscosity, c_p is heat at constant pressure and k the thermal diffusivity. In this work, numerical simulations are conducted for different Reynolds numbers (Re = 1 - 500), while keeping the Prandtl number fixed at Pr = 0.7. Both heat and fluid flow characteristics like the drag C_d and lift C_ℓ coefficients, recirculation behind the cylinder, streamline and isotherm pattern, average Nusselt number on the cylinder surface are presented and compared with previous result in the literature. In this case, the angle formed by the segment joining the centers of the two cylinders and the axis of the abscissa is zero.

5.1 Description of the problem and boundary conditions

In the Fig. 1, the two cylinders are identical and fixed with the same diameters, maintained in “tandem” (cylinders in line) with downstream of the cylinder A. The cylinders are confined to a channel with free flow, with uniform velocity (U_∞) and constant temperature (T_c (>T_∞)). The horizontal and vertical spacing between the cylinders are fixed in L_u = 16.5 d and L_d = 19.5 d, respectively. These values are chosen to reduce the effect of boundary conditions on the inlet and outlet relative to the flow patter and the cylinder boundary.

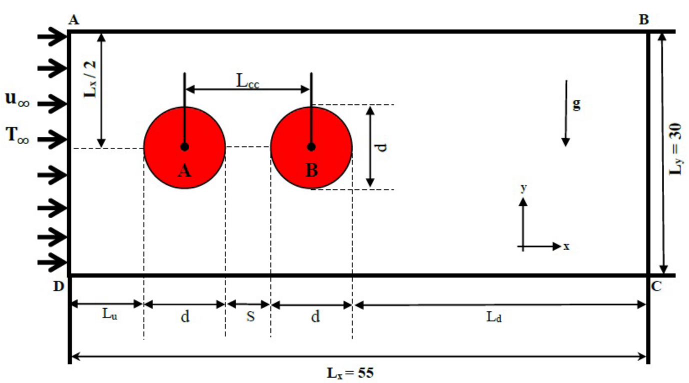

Figure 1: Illustration of the computational domain with two cylinders in tandem configuration.

The drag (C_d) and lift (C_ℓ) coefficients for the calculation of each cylinder are performed as follows:

$$C_d = C_{dp} + C_{dv} = \frac{2F_d}{\rho U_\infty^2 D}, \tag{37}$$

$$C_\ell = C_{\ell p} + C_{\ell v} = \frac{2F_\ell}{\rho U_\infty^2 D}, \tag{38}$$

where, $C_{\ell p}$ and $C_{\ell v}$ represent the lift coefficients due pressure and viscous forces, respectively. In a similar way, C_{dp} and C_{dv}, represent the drag coefficients due to the pressure and viscous forces. The terms, F_d and F_ℓ are forces of drag and lift, respectively, acting on the surface of the cylinder. Thus, the drag and lift coefficients can be obtained from the expressions:

$$\begin{cases} C_{dp} = 2\int_0^1 (p_f - p_r)\, dy\,, \\ C_{dv} = \dfrac{2}{Re}\int_0^1 \left[\left\{\left(\dfrac{\partial u}{\partial y}\right)_s + \left(\dfrac{\partial u}{\partial y}\right)_i\right\} dx + \left\{\left(\dfrac{\partial u}{\partial x}\right)_f + \left(\dfrac{\partial u}{\partial x}\right)_r\right\} dy\right], \end{cases} \tag{39}$$

$$\begin{cases} C_{lp} = 2\int_0^1 (p_i - p_s)\, dy\,, \\ C_{\ell v} = \dfrac{2}{Re}\int_0^1 \left[\left\{\left(\dfrac{\partial u}{\partial y}\right)_f + \left(\dfrac{\partial u}{\partial y}\right)_b\right\} dx + \left\{\left(\dfrac{\partial u}{\partial x}\right)_t + \left(\dfrac{\partial u}{\partial x}\right)_i\right\} dy\right], \end{cases} \tag{40}$$

5.2 Flow fields for *Re* = 500 and *Rí* = 0 in cylinders in tandem with forced convection

The Figs. (2) and (3) present simplified fields of temperature, pressure, effective viscosity, vorticity, isothermal lines, and aerodynamics coefficients, C_d and C_ℓ, for the flow around cylinder tandem, for Reynolds and Richardson numbers, equals to 500 and 0, respectively.

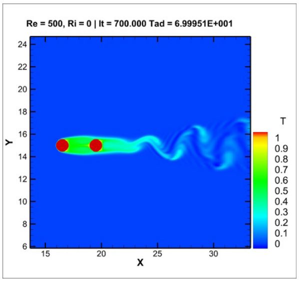

(a)

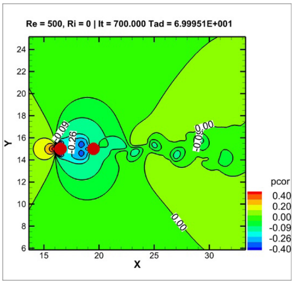

(b)

Figure 2: Smagorinsky model for simplified fields of (a) temperature, and (b) pressure for cylinders, for *Re* = 500 with *Ri* = 0.

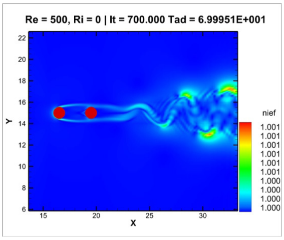

(c)

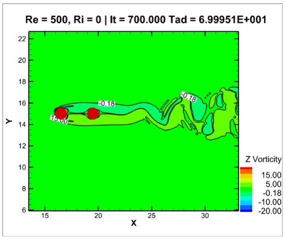

(d)

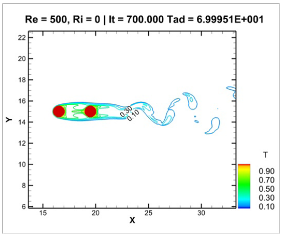

(e)

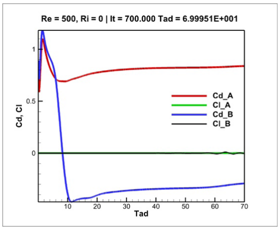

(f)

Figure 3: Smagorinsky model for simplified fields of (c) effective viscosity (d) vorticity (d) € isotherms lines and Drag (C_d) and Lift C_ℓ coefficients for cylinders, for Re = 500 with R_i = 0.

The main results for the simulations can be summarized as follows:

- A wake forms upstream of the second cylinder, but it needs to be checked whether it can be decreased or suppressed with the increase of the distance between the cylinders;
- The isothermal lines reflect the same behavior of the pattern of the streamlines (current lines);
- The average Nusselt number increase for Re = 500 for different value of R_i, even keeping the distance between the cylinders;
- The thermal buoyancy is suppressed in the recirculation zones of the tandem cylinders, even with a mounting angle;
- The thermal buoyancy tends to in the recirculation zones of the tandem cylinders, even with a mounting angle;
- The thermal buoyancy tends to increase the coefficient of drag and the average Nusselt number of the cylinder more than the second.

Re	L_{cc}/d	$C_{d,1}$	$C_{l,1}$	St_m	$C_{d,2}$	$C_{l,2}$
100	2	1,222	±0,0072	-	±0,0008	±0,0255
	2,5	1,386±0,011[a]	±0,37	0,169	-0,075	0
	3	1,202	0	-	-0,045	0,0011±0,004
	4	1,342±0,0243	±0,475	0,153	0,761±0,200	±1,452
200	2	1,03±0,0004	±0,031	-	-0,18±0,0033	±0,14
		0,89±0,05[b]	±0,20	0,130	-0,21±0,15	-
		1,03[c]	-	0,130	-0,17	-
	3	1,048±0,021	±0,026	0,130	-0,53±0,012	±0,266
500	3	0,8041±0,015	±1,343	0,216	-0,357±0,008	-4,715±0,008

Table 1: Flow parameters for *Re* = 100,200 and 500 compared to data available in the literature.

5.3 Variations of the Nusselt number

One of the main purposes of the heat transfer calculations involving cylinders is to determine the local and total transfer around isothermal cylinders. The effect of the flow, especially with respect to the heat transfer, can be better observed by analyzing the local heat transfer coefficient, also known as the Nusselt local number. In the Fig. (4), for different Richardson numbers, the distributions of Nusselt numbers along the perimeter of the upstream and downstream cylinders are provided. For L_{cc}/d =3, *Re* = 100, *Re* = 200 and *Re* = 500, for different Richardson numbers, the local distributions of the Nusselt numbers along the perimeter of the upstream and downstream cylinders are provided. For L_{cc}/d =3, although the local profile of the Nusselt number of the upstream cylinder is similar to that of an isolated cylinder, the downstream cylinder has completely different characteristics, as the transfer rate is closely related to the flow, the local minimum rates of heat transfer appear at the front back stagnation points of the downstream cylinder, where the magnitude of velocities are relatively small.

This, in Fig. (11-(a)), the maximum heat transfer from the downstream cylinder is exhibited with a double protuberance in $\theta \approx 57^{\circ}$ and $\theta \approx 265^{\circ}$ from the cylinder wall, where thermal layers (also known as thermal plumes) and hydrodynamics becomes thinner. The formation of vortices in the downstream region of the cylinder coincides with the oscillations of the average Nusselt number from large amplitude to low amplitude during a vortex release period for L_{cc}/d =3 and *Re* = 500 for different values of *Rí*, as see in Fig. (11-(b)). It is important to note that although the Nusselt's local distribution of the downstream cylinders resembles that of the upstream cylinder, typified as large protuberance, its magnitude is smaller than of the upstream cylinder, indicating smaller heat-to-cylinder conversion to downstream.

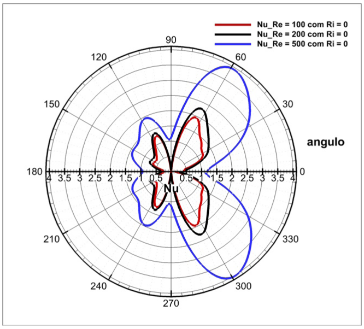

(a)

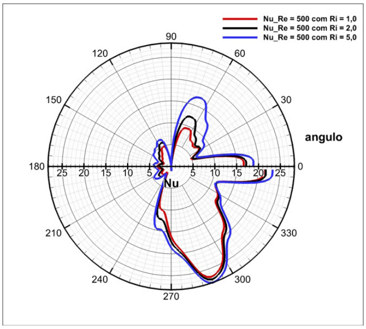

(b)

Figure 4: Local variation of the Nusselt number to the same dimensionless instants: (a) - *Re* = 100, *Re* = 200 and *Re* = 500 for *Rí* = 0 (forced convection) and (b) - *Re* = 500 for *Rí* = 1.0, *Rí* = 2.0 and *Rí* = 5.0 (natural convection).

6 I CONCLUSIONS

In this work, a boundary condition-enforced immersed boundary method is developed for simulations of heat and mass transfer problems. The effect of thermal boundaries in the flow and temperature fields considered through the velocity and temperature corrections. The temperature corrections is evaluated implicitly in such a way that the temperature at the immersed boundary, interpolated from the corrected temperature field, satisfies the physical boundary conditions.

For the momentum transfer between the immersed body and the surrounding fluid, the additional momentum forcing obtained by using the forcing term is added to the fluid-body equation. To model the onset turbulence, the Smagorinsky and Spalart-Allmaras models are used. The first model used LES methodology and is based on local equilibrium hypothesis for small scales associated with the Boussinesq hypothesis, such that the energy injected into the spectrum of the turbulence balances the energy dissipated by convective effects. The second model used the URANS concept, with only one transport equation for turbulence viscosity, being calibrated in pressure gradient layers. A computational code was developed to implement the methodology mentioned herein in order to analyze the combination of the heat-transfer phenomena in the turbulence for the thermofluid dynamics interaction around isothermal complex geometries. The agreement of the results with the available data in the literature validates the numerical method.

REFERENCES

1. Badr, H. M., & Dennis, S. C. R. (1985). **Time-dependent viscous flow past an impulsively started rotating and translating circular cylinder**. *Journal of Fluid Mechanics*, *158*, 447-488.

2. Badr, H. M., Coutanceau, M., Dennis, S. C. R., & Menard, C. (1990). **Unsteady flow past a rotating circular cylinder at Reynolds numbers 10^3 and 10^4**. *Journal of Fluid Mechanics*, *220*, 459-484.

3. Sharma, V., and Dhiman A. K., Heat **Transfer from a Rotating Circular Cylinder in The Steady Regime: Effects of Prandtl Number**. Thermal Science, v.16, n.01, pp. 79-91, 2012.

4. Park, S. G., Chang, C. B., Kim, B. and Sung, H. J. (2017). **Simulation of Fluid-Flexible Body Interaction with Heat Transfer**. Int. J. Heat Mass Transfer, 110, 20–33.

5. Santos, R. D., Gama, S.M., & Camacho, R. G. (2018). **Two-Dimensional Simulation of the Navier-Stokes Equations for Laminar and Turbulent Flow around a Heated Square Cylinder with Forced Convection.** Applied Mathematics, 9(03), 291–312.

6. Silva, A. L. E., Silveira-Neto, A. and Damasceno, J. J. R. (2003). **Numerical Simulation of Two-Dimensional Flows over a Circular Cylinder using the Immersed Boundary Method.** J. Comput. Phys., 189, 351–370.

7. PESKIN, C. S. **Numerical Analysis Of Blood Flow In The Heart**. Journal of Computational Physics. v.25, pp. 220-252, 1977.

8. Juric, D., **Computation of Phase Change**, Ph. D. Thesis, Mech. Eng. Univ. of Michigan, USA, 1996.

9. Smagorinsky, J. (1963) **General Circulation Experiments with the Primitive Equations: I. The Basic Experiment**. Monthly Weather Review, 91, 99–164.

10. Spalart, P. & Allmaras, S. (1992). **A One-Equation Turbulence Model for Aerodynamics Flows.** Recherce Aeropatiale, No. 1, 5–21.

11. Schneider, G. E.; Zedan, M. **A Modified Strongly Implicit Procedure For the Numerical Solution of Field Problems**. Numerical Heat Transfer, v. 4, n.01, pp. 1-19, 1981.

ÍNDICE REMISSIVO

S

T

U

INVESTIGAÇÃO, CONSTRUÇÃO E DIFUSÃO DO CONHECIMENTO EM MATEMÁTICA 2

www.atenaeditora.com.br
contato@atenaeditora.com.br
@atenaeditora
www.facebook.com/atenaeditora.com.br

Atena Editora
Ano 2020

INVESTIGAÇÃO, CONSTRUÇÃO E DIFUSÃO DO CONHECIMENTO EM MATEMÁTICA 2

www.atenaeditora.com.br
contato@atenaeditora.com.br
@atenaeditora
www.facebook.com/atenaeditora.com.br

Atena Editora
Ano 2020